Journal of Hydrology 588 (2020) 124996

Contents lists available at ScienceDirect

Journal of Hydrology

journal homepage: www.elsevier.com/locate/jhydrol

Research papers

The coupling impact of climate change on streamflow complexity in the headwater area of the northeastern Tibetan Plateau across multiple timescales

Shi Shen[a,b,c], Changqing Song[a,b,c,*], Changxiu Cheng[a,b,c,d], Sijing Ye[a,b,c]

[a] State Key Laboratory of Earth Surface Processes and Resource Ecology, Beijing Normal University, Beijing 100875, China
[b] Faculty of Geographical Science, Beijing Normal University, Beijing 100875, China
[c] Center for Geodata and Analysis, Beijing Normal University, Beijing 100875, China
[d] National Tibetan Plateau Data Center, Beijing 100101, China

ARTICLE INFO

This manuscript was handled by Dr Emmanouil Anagnostou, Editor-in-Chief

Keywords:
Climate change
Streamflow complexity
Permutation entropy
Wavelet analysis
Tibetan plateau

ABSTRACT

The streamflow from the headwater areas of the Tibetan Plateau (TP) provides critical support for downstream regions, yet understanding of the streamflow complexity on the TP, which is essential for hydrological modeling and water resource management, remains scarce. This study aims to measure streamflow complexity in the headwater areas of the TP and investigate the coupling effects of climatic variables (i.e., precipitation and air temperature) on the streamflow complexity across multiple timescales. Using daily streamflow records, we employ permutation entropy as the measure of annual streamflow complexity in the upper Heihe River (UHR) watershed in the northeastern TP from 1960 to 2014. Additionally, wavelet coherence is applied to evaluate the impact of climate (i.e., precipitation and temperature) change. Our results show: (1) due to climate change, streamflow complexity has significantly increased since 1972 in the UHR watershed; (2) the periods of warmer and wetter weather have a longer-term influence on streamflow complexity. Specifically, before 1972, dryer, colder weather in the TP would significantly affect the complexity of the streamflow every three to four years, but after that date, these climatic events occurred less frequently, with gaps of between eight and twelve years, during which the weather was much warmer and wetter; and (3) the influence of precipitation on the streamflow complexity decreased, while that of air temperature increased. Therefore, the impact of climate change on streamflow complexity relating to the dynamic structure of streamflow should be regarded as significant to the work of hydrologists and water resource management agencies.

1. Introduction

The Tibetan Plateau (TP), sometimes known as the "Asian water tower," is the origin of the major Asian rivers, Yangtze, Yellow, Indus, and Ganges (Xu et al., 2008). It is also one of the most sensitive and vulnerable regions on earth with regard to climate change (Brown et al., 2007; Immerzeel et al., 2010). Streamflow from the headwater areas on the TP continuously provides essential water resources that support the habitation, socio-economic development, and ecosystem services of 1.4 billion people (Bibi et al., 2018; Milly et al., 2005; Oki and Kanae, 2006). Affected by anthropogenic activity, climate change, and the landscape, streamflow exhibits typical nonlinear behavior, which varies in both time and space (Parajka et al., 2013; Sivakumar, 2009; Sivakumar and Singh, 2012; Zhang et al., 2016; Zhang et al., 2017). Thus, the term "streamflow" represents a typical complex hydrological system. "Streamflow complexity" is defined as the variability and uncertainty of streamflow and reflects the dynamic structure of streamflow (Singh, 1997; Sivakumar and Singh, 2012). Therefore, measuring streamflow complexity in the TP, and investigating its temporal changes, is vital to improving our understanding of the hydrometeorological process, not just in the affected areas but across the globe.

There have been numerous efforts to study streamflow complexity in recent decades, ranging in scale from a single river to an entire continent (Huang et al., 2017; Mihailović et al., 2019; Sen, 2009; Serinaldi et al., 2014; Srivalli et al., 2019). Most studies concentrate on streamflow complexity in the middle and downstream areas (Huang et al., 2011; Srivalli et al., 2019; Stosic et al., 2016; Wang et al., 2020; Zhang et al., 2012) rather than at the headwater, and information on streamflow complexity at headwaters remains scarce, though these

* Corresponding author at: State Key Laboratory of Earth Surface Processes and Resource Ecology, Beijing Normal University, Beijing 100875, China.
E-mail addresses: shens@bnu.edu.cn (S. Shen), songcq@bnu.edu.cn (C. Song), chengcx@bnu.edu.cn (C. Cheng), yesj@bnu.edu.cn (S. Ye).

https://doi.org/10.1016/j.jhydrol.2020.124996
Received 2 March 2020; Received in revised form 14 April 2020; Accepted 20 April 2020
Available online 11 May 2020
0022-1694/

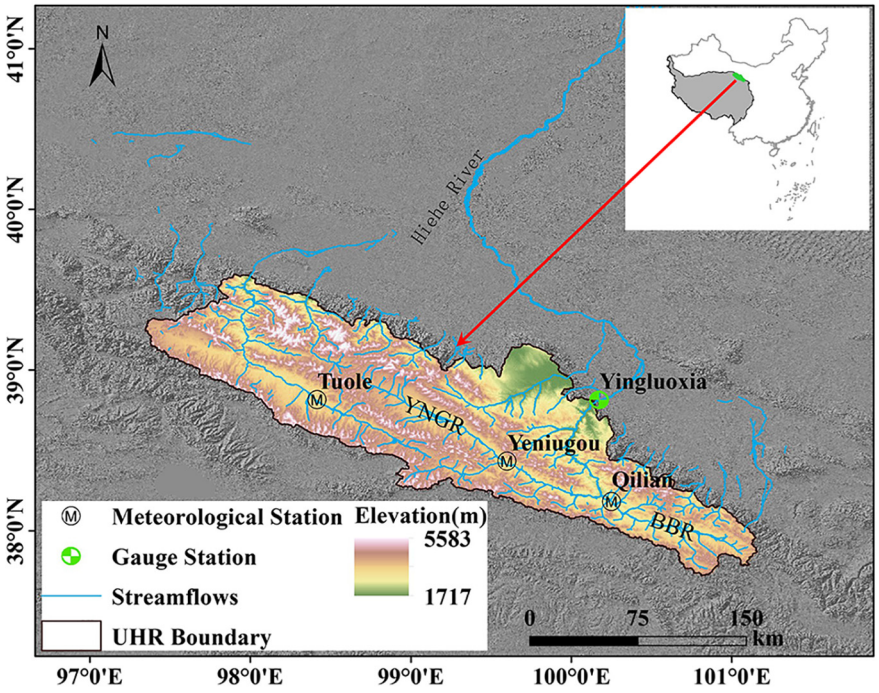

Fig. 1. The upper Heihe River watershed, the position of the gauge station, and distribution of the meteorological stations.

areas represent a critical stage in the hydrological cycle and land-surface system.

Meanwhile, existing work looks at how streamflow complexity is affected by human activity such as reservoir operations (Huang et al., 2011; Liu et al., 2017; Zhang et al., 2019a), dam construction (Luo et al., 2019; Stosic et al., 2016; Zhang et al., 2012; Zhou et al., 2012), and land use/land cover changes (Li and Zhang, 2008; Liu et al., 2018). In addition, researchers have used streamflow complexity as a metric for the evaluation of hydrological changes (Jovanovic et al., 2017), catchment classification (Sivakumar and Singh, 2012), and basin complexity (Pande and Moayeri, 2018). However, the effect of climate change on the streamcomplexity is unclear.

The streamflow complexity of the TP is significant due to the mountainous landscape and sophisticated cryospheric changes in this region. The headwater areas of the TP are typical alpine watersheds with a wide distribution of permafrost, glaciers, and snow-covered mountains. The snow and glacier melt not only provide critical water resource to the downstream areas in dry seasons but also add to the streamflow complexity (Huss and Hock, 2018; Singh and Bengtsson, 2005; Wulf et al., 2016). The lack of *in situ* observations and measurements has restricted our understanding of the streamflow in mountainous glacial alpine watersheds (Wang et al., 2019). To improve our understanding of the hydrological system in the TP, it is crucial to measure the streamflow complexity in the headwater areas of this region.

Furthermore, our understanding of the influence of climate change on streamflow complexity is also insufficient. The TP as one of the world's regions with the most significant climate change (Chen et al., 2015; Kuang and Jiao, 2016), is still lacking studies that investigated the impact of climate change on sections of the streamflow complexity in the TP. Observation data analyses and model simulations show that the air temperature in the TP has increased significantly during the last 50 years (Kuang and Jiao, 2016; You et al., 2016; Zhong et al., 2011), and the warming rate is twice the global average over the same period (Chen et al., 2015). Meanwhile, despite the substantial spatial heterogeneity of precipitation on the TP, the overall precipitation has also slightly increased (Kuang and Jiao, 2016). Compared with the air temperature, the impact of precipitation on the streamflow complexity has attracted more attention because of its significant role in the hydrological cycle (Chou, 2014; Huang et al., 2011; Pan et al., 2012). However, the air temperature is also likely to affect the hydrological cycle by changing the processes in the cryosphere, biosphere, and atmosphere (Cuo et al., 2015; Deng et al., 2017; Gao et al., 2018). Investigating the impact of climate (i.e., air temperature and precipitation) change on the streamflow complexity will also expand our knowledge of hydrothermal interaction in cold and arid regions.

The impact of climate variables (i.e., precipitation and air temperature) on streamflow complexity also has multi-timescale characteristics (Liu et al., 2019). Chou found that the complexity of the rainfall–runoff coefficient series, which indicates the precipitation–streamflow relationship, increased along with the increase of scale factor (Chou, 2012). Huang et al. (2017) analyzed a streamflow series and also found that the streamflow complexity increased from daily to seasonal timescales. Streamflow, precipitation, and air temperature individually also show different characteristics at diurnal, monthly, seasonal, annual, and decadal timescales (Büntgen et al., 2005; Jones et al., 1999; Sang et al., 2009; Sharifi et al., 2018; Su et al., 2017). Given the lack of relevant works, new research probing the influence of precipitation and air temperature at multiple timescales is necessary for additional insight into streamflow complexity.

This study has two main objectives: (1) to measure the streamflow complexity and understand its changes in the headwater area of the TP; and (2) to investigate the impact of climate change on the streamflow complexity at multiple timescales. To achieve these objectives, we used a capable and robust entropy-based measure, permutation entropy (PE) to quantifying streamflow complexity in the TP. We also used the Mann–Kendall test to evaluate the trends and change points of the complexity, and wavelet transform coherence (WTC), which is a scale-dependent and reliable method to analyze localized, scattered periodicities of the influence of precipitation and air temperature. In particular, we focused on the upper Heihe River (UHR) basin, on the northeast TP. The streamflow from the UHR basin accounts for approximately 70% of the total streamflow in the Heihe River.

The paper is organized as follows. In Section 2, we introduce the

study area and data; in Section 3 we describe PE, the Mann–Kendall test, and WTC; the main results of this study are presented in Section 4; and finally, we provide discussion and conclusions in Sections 5 and 6, respectively.

2. Study area and data

2.1. Study area

As the headwater of the Heihe River basin (HRB), the UHR watershed (Fig. 1) provides most of the water supply for the HRB–the second-largest inland river in China. The two tributaries of the UHR, the Babaohe River (BBR) and the Yeniugou River (YNGR), converge into the mainstream and cross the Qilian Mountains at the Yingluoxia (YLX) gauging station into the middle reaches of the Heihe River. The average annual mean temperature in the UHR basin ranges from −9°C to 5 °C, and the average annual precipitation exceeds 400 mm.

The UHR watershed is a typical alpine-glacial region with wide distribution of permafrost and seasonal frozen ground. It locates in the Qilian Mountains on the northeastern edge of the TP and has experienced significant climate change. The climate in the UHR basin has been getting warmer and wetter in recent decades. Tree ring-based reconstructed temperature series suggest that the 20th century was the warmest 100 years in the area's history (Wang et al., 2016). Moreover, the upward trend of the air temperature has become steeper since the 1980 s (Wang et al., 2010). Meanwhile, precipitation has also experienced a significant increase at a rate of 1.04 mm/year from 1961 to 2016 (Zhong et al., 2019). In addition, glacier coverage areas in the UHR have declined from 66.3 km^2 in 1990 to 13.37 km^2 in 2010, generally attributed to climate change (Cai et al., 2014). The lower limit of permafrost has climbed from 100 to 200 m, and the permafrost has retreated 10–20 km along the major highways of the YNGR watershed since 1985 (Wang et al., 2017). The maximum thickness of the seasonal frozen ground has also decreased by about 20 cm (Wang et al., 2015).

2.2. Data

Data used in this study include daily streamflow records from 1960 to 2014 and climatic data (i.e., precipitation and air temperature) from 1960 to 2014. Daily streamflow records in the Yingluoxia gauge station (coordinates: 38°49′12″N, 100°10′48″E; elevation:1700 m) were obtained from the Environmental and Ecological Science Data Center for West China (http://www.heihedata.org). The climatic data consists of the daily mean air temperature and daily cumulative precipitation at three national meteorological stations: Qilian (QL; coordinates: 38°10′48″N 100°15′0″E; elevation: 2787.4 m); Yeniugou (YNG; coordinates: 38°45′48″N,99°36′00″E; elevation: 3314 m); and Tuole (TL; coordinates: 38°49′12″N, 98°25′12″E; elevation: 3367 m). These were downloaded from the National Meteorological Information Center of the China Meteorological Administration (http://data.cma.cn). It is worth noting that the precipitation data in this article include both rainfall and snowfall. Because of a lack of observation data for precipitation, air temperature, or streamflow in individual years, we chose 1960–2014 as the joint period.

3. Methods

3.1. Permutation entropy

PE was proposed to finely measure the complexity of time series by Bandt and Pompe (2002). Having no requirement for assumptions on linearity or normality, entropy theory has been widely used to study and understand hydrological systems (Singh, 1997; Singh, 2011). In recent decades, various entropy methods have been employed to measure streamflow complexity, such as sample entropy (Huang et al., 2011; Wang et al., 2020), multi-scale sample entropy (Huang et al., 2017; Li and Zhang, 2008; Zhang et al., 2012), wavelet-based entropy (Sang et al., 2011), Shannon entropy (Castillo et al., 2015; Krasovskaia, 1995), and Kolmogorov entropy (Mihailović et al., 2014). In contrast to these entropy measures, PE considers the ordinal pattern of the values in a time series (Stosic et al., 2016). Due to its simplicity and robustness, PE has attracted attention from researchers and been applied in hydrology and other domains, including finance (Hou et al., 2017; Zunino et al., 2009), meteorology (Zhang et al., 2019b), and bioinformatics (Zanin et al., 2012). The calculation process of PE can be described as follows.

A given time series $\{s(i), i = 1, 2, \cdots, N\}$, $S(i)$ represents the embedding vector $[s(i), s(i+\tau), \cdots, s(i+(d-1)\tau)]$, where d denotes the embedding dimension and τ indicates the delay time. We can sort the elements in vector $S(i)$ in ascending order as $[s(i+(j_1-1)\tau) \le x(i+(j_2-1)\tau \le \cdots \le s(i+(j_d-1)\tau)]$, while the series $\{j_1, j_2, \cdots, j_d\}$ denotes the indices of elements in $S(i)$. In particular, when there is equality in a time series, we can sort them according to their original orders. For instance, if $s(i+(j_{t1}-1)\tau) = s(i+(j_{t2})\tau)$ and $j_{t1} < j_{t2}$, then these two elements can be sorted as $s(i+(j_{t1}-1)\tau) \le s(i+(j_{t2})\tau)$. Therefore, the original vector $S(i)$ can be mapped to a symbolic permutation $\Pi = [j_1, j_2, \cdots, j_d]$, which is one of $d!$ possible permutations. Assuming the number of unique permutations is K, the probability of each Π denotes as $\{p_1, p_2, \cdots, p_h\}$. The PE of the time series Si is computed as

$$H(d) = -\sum_{h=1}^{K} p_h ln P_h$$

When $p_1 = p_2 = \cdots = p_h = 1/\ln(d!)$, $H(d)$has the maximum value$ln(d!)$. Therefore, the PE can be normalized as

$$PE(d)\frac{H(d)}{ln(d!)}$$

A normalized PE is restricted between 0 and 1. PE close to zero means the times series is a more deterministic increasing or decreasing series. Conversely, a PE close to one means the time series is more random and chaotic.

Before computing the PE of a time series, it is split into non-overlapping segments of short length, and then the PE of each segment is computed. Changes in the PE measurements can be investigated to explore dynamic change in a time series. The embedding dimension d usually depends on the observed phenomenon. For useful statistics, it is generally recommended to choose the maximum d according to $N > 5d!$ (Ribeiro et al., 2012). For this study, we computed the PE from the daily streamflow records of the Yingluoxia gauge station for each calendar year. The embedding dimension d and delay time τ were set to 4 and 1, respectively.

3.2. Mann–Kendall test

The Mann–Kendall test (M−K test) is a nonparametric and robust method for detecting trends in time series, originally proposed by Mann (1945) and improved by Kendall (1975). Since it has been widely applied and verified in hydrological studies, we employed it to identify the trends from the streamflow PE series. A detailed description of the M−K test can be found in Hamed and Ramachandra Rao (1998) and Sang et al. (2014).

3.3. Wavelet transform coherence

Wavelet transform coherence (WTC), which describes the coherence of two time series, can be regarded as a localized correlation coefficient between two time series in time and frequency space (Cazelles et al., 2008; Grinsted et al., 2004; Torrence and Compo, 1998). Torrence and Webster (1999) defined the WTC of two times series X and Y as follows

$$R_n^2(s) = \frac{|S(s^{-1}W_n^{XY}(s))|^2}{S(s^{-1}|W_n^X(s)|^2)\bullet S(s^{-1}|W_n^Y(s)|^2)}$$

where $W_n^X(s)$ and $W_n^Y(s)$ denote the wavelet transformation of X and Y, respectively. $W_n^{XY}(s)$ denotes the cross-wavelet transformation of X and Y. S is a smoothing operator depending on the wavelet used. In general, the smoothing operator S for a wavelet is written as

$$S(W) = S_s(S_t(W_n(s)))$$

in which the S_s and S_t are smoothing along the wavelet scale axis and the time, respectively. $W_n(s)$ denotes the wavelet transformation of a time series where s indicates the wavelet scale factor. $R_n^2(s)$ denotes the value of WTC and ranges between 0 and 1. As with the correlation coefficient, a value equal to zero depicts an independent two time series, while the value equal to one depicts that the two times series perfectly co-vary. We estimated the statistical significance level of the WTC against a first-order autoregressive red noise series assumption using Monte Carlo methods. In this study, the significance level was 0.05. It is worth noting that only the values outside the cone of influence (COI) are taken to estimate the significance level for each scale. The COI indicates the areas in the wavelet coherence likely to be impacted by the edge effect artifacts.

We chose the Morlet wavelet as the mother wavelet function owing to its balance between time and frequency (Grinsted et al., 2004). More details of this method of computing WTC can be found in the work of Grinsted et al. (2004).

4. Results

4.1. Streamflow complexity in the UHR watershed

We applied a normalized PE measure on the daily streamflow records, daily mean air temperature, and daily cumulative precipitation in the UHR watershed to each year from 1960 to 2014 (Fig. 2). In Fig. 2a, the solid cyan, red, and yellow lines represent the annual PE of the air temperature. The cyan, red, and yellow dashed lines represent the annual PE of the precipitation. The blue line represents the PE of the streamflow.

From Fig. 2, it can be seen that the complexity of the streamflow in the UHR was a significantly nonstationary process that had a turning point in the year 1972. The M − K test result showed an increasing trend in the streamflow complexity (UF larger than 0 in Fig. 2) with the last changing point in 1972. There was an increasingly fluctuating trend in most years after 1980, in which the UF value was larger than the threshold 1.96. This phenomenon coincided with increasing air temperature in the eastern TP since the 1980s (Kuang and Jiao, 2016).

Therefore, we partitioned the PE series into two different periods: from 1960 to 1972, and from 1973 to 2014. In the first period, the PE of the streamflow experienced a process of dramatic increase followed by a sharp decrease. The average PE value during this period was 0.84. However, the PE values after 1972 were higher and relatively stable. The average PE value after 1972 was 0.89. This result suggests that after 1972 the dynamic features and structures of the streamflow in the UHR become more complex.

Overall, the complexity of the streamflow is essentially the dynamic between air temperature and precipitation. Notably, after 1972, the PE of the streamflow was closer to that of the air temperature than before, implying that the influence of the air temperature in the UHR watershed on the streamflow complexity may have increased after 1972. Meanwhile, we found that even the lowest PE (0.73) of streamflow was still higher than the PE of precipitation (i.e., QL:0.61, YNG: 0.65; TL: 0.51) in the corresponding year (1961). Additionally, it is worth noting that the PE troughs of streamflow and precipitation did not always occur at the same time. The upward results indicate that the streamflow was a more complex, uncertain, and chaotic process than the precipitation in the UHR watershed.

We summarized the statistics (Table 1) and drew boxplots (Fig. 3) of the PE of streamflow before and after 1972. Before 1972, the mean, median, and quantiles of the PE of streamflow were located between those of air temperature and precipitation. Moreover, the standard deviation of the streamflow's complexity was close to that of the precipitation, while the streamflow had the most extensive range of complexity, which indicates that the streamflow complexity varied greatly, more dramatically than the air temperature and precipitation, and its variation was more similar to the complexity of the precipitation.

After 1972, however, it is clear that the statistics of the PE of streamflow were higher and more stable than before, and the complexity of the air temperature remained steady while the range of the complexity of precipitation expanded. This result implies that the streamflow complexity had increased and then stabilized in a "stale" phase after 1972. Although the complexity of the air temperature was relatively stable, the complexity of the precipitation varied greatly. These changes in the streamflow complexity imply that the dynamic structure and uncertainty of streamflow may have changed to more complex and higher.

4.2. Impact of air temperature on streamflow complexity at multiple timescales

To investigate the impact of the air temperature on the streamflow complexity, we applied a WTC analysis of the annual mean air temperature and annual normalized PE of the streamflow. Fig. 4 shows the result. The black contours denote the 0.05 significance level against the red noise. The shadow region denotes the COI. The small arrows denote the relative phase relationship with in-phase pointing right and anti-phase pointing left.

In Fig. 4, two different bands of wavelet coherence show between the streamflow's complexity and air temperature. For the streamflow complexity, the wavelet coherence with the air temperature at three stations depicts high interannual covariance over a series of 2–4-year periods between 1962 and 1970 with the in-phase. However, the wavelet coherence between the air temperature and streamflow complexity had a quasi-decadal period during 1994–2008 with the anti-phase, with half of this region inside the COI. Considering the 5% high significance level and the vast region of wavelet coherence, this quasi-decadal period can extend to 1988–2012.

This result indicates that the influence of air temperature on the streamflow complexity changes from a short timescale to a long timescale. The change from in-phase to anti-phase indicates that the relationship between the air temperature and the streamflow complexity had to transform from a positive to a negative relation. Additionally, we noticed that the WTC disappeared at TL station (Fig. 4c), which may imply that the role of air temperature in the marginal area of the UHR watershed was weakening. Because air temperature can accelerate the glacier melting rate, permafrost degradation, and the ratio of solid and liquid precipitation, the indirect impact of temperature on the streamflow changed to more significant at the long timescale. But at the marginal area, the impact of temperature was weak due to the high latitude.

4.3. Impact of precipitation on the streamflow complexity at multiple timescales

We also applied a WTC analysis to investigate the impact of precipitation on the streamflow complexity at multiple timescales. The annual cumulative precipitation and the annual normalized PE of streamflow were used. The result of the WTC between the precipitation and the streamflow complexity is shown in Fig. 5.

The wavelet coherence between the precipitation and the streamflow complexity also exhibits two discrete regions. There is a 2–4-year band of high covariance between 1964 and 1972, and the down arrows indicate that the precipitation led to a streamflow complexity of

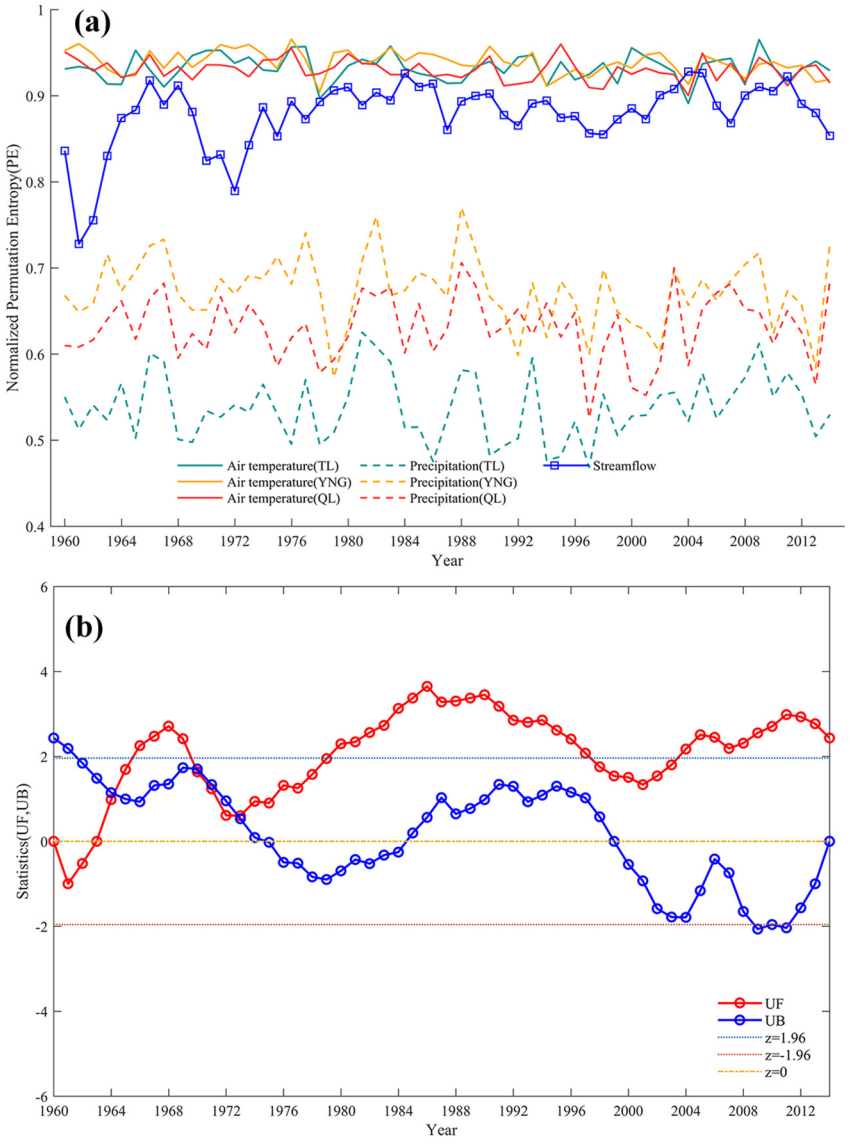

Fig. 2. (a) The interannual variations of the PE of streamflow at Yingluoxia gauge station, the PE of air temperature, and the PE of precipitation at TL, YNG, and QL meteorological stations. (b) M − K test of streamflow complexity.

Table 1
The statistics of the PE of streamflow, air temperature, and precipitation.

Years	Permutation entropy of	Station	Mean	Std Dev	Range
1960 to 1972	Streamflow	YLX	0.84	0.06	0.19
	Air temperature	QL	0.93	0.01	0.03
		YNG	0.94	0.01	0.04
		TL	0.93	0.01	0.04
	Precipitation	QL	0.63	0.03	0.09
		YNG	0.68	0.03	0.08
		TL	0.54	0.03	0.10
1973 to 2014	Streamflow	YLX	0.89	0.02	0.09
	Air temperature	QL	0.93	0.01	0.06
		YNG	0.94	0.01	0.06
		TL	0.93	0.02	0.07
	Precipitation	QL	0.63	0.04	0.18
		YNG	0.67	0.04	0.20
		TL	0.54	0.04	0.16

approximately 90° (about 0.5–1 year). The WTC between the precipitation and the streamflow complexity also had a long-term 4–6-year band between 1988 and 2006, and the up arrows indicate that the precipitation led to a streamflow complexity of approximately 270° (about 3–4.5 years). The results show that although the degree of covariance between the precipitation and the streamflow complexity slightly weakened after 1972, the timescales and range both substantially extended. In addition, we found that the influence of precipitation at TL station on the streamflow complexity was significantly weaker than that at QL and YNG stations. This result is almost the same as the air temperature and may imply that the weakening impact of climate on the marginal area of the UHR maybe not be mere chance.

4.4. Climate change regarding the streamflow complexity

To further investigate the possible impact of climate change on the observed shifts in streamflow complexity, we conducted a comparative analysis between two specific periods. The WTC analysis, as mentioned above, indicated that air temperature and precipitation both influence

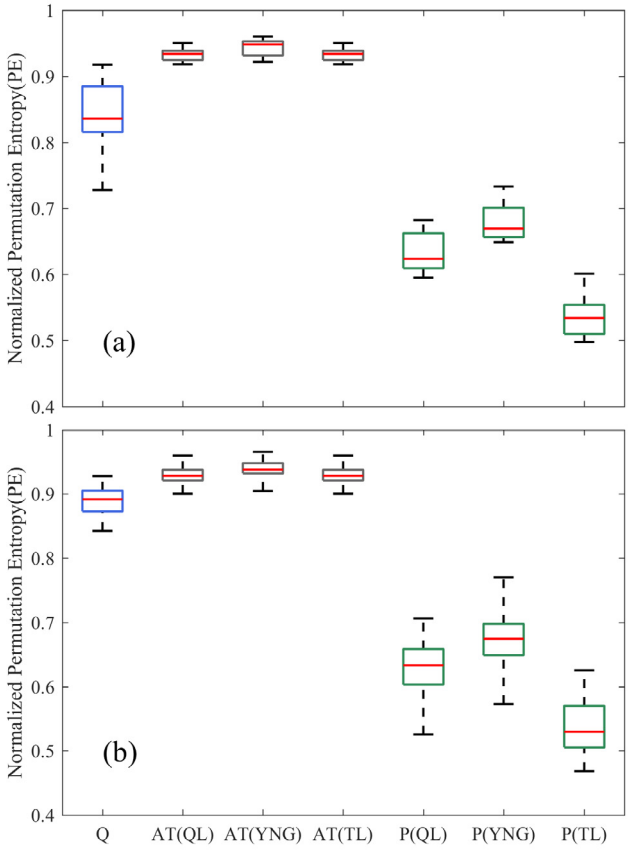

Fig. 3. Boxplots of the PE of streamflow (Q), air temperature (AT), and precipitation (P) during 1960–1972 (a), and 1973–2014 (b).

streamflow complexity, but their different phases show that the influence changed before and after 1971. According to the regions with high WTCs of precipitation and air temperature, we chose 1964–1970 and 1988–2012 for our two comparative time periods.

To illustrate the air temperature and precipitation changes in the UHR watershed, the annual mean air temperature and annual accumulative precipitation anomalies relative to the 1960–2014 base period were calculated. Fig. 6 shows the interannual variations of the air temperature and precipitation anomalies, and the shadow regions indicate the two time periods with high WTCs. Before 1972, most air temperature and precipitation anomalies at the three stations were negative except for some discrete years. Additionally, two low air temperature anomalies appeared during the 1964–1970 period with high WTCs. The results demonstrate that a coupling impact of unusual low temperature and normal precipitation may create variations in streamflow complexity.

However, more continuous and marked anomalies of air temperature and precipitation occurred after 1972, and especially after 1988. Besides, there were clear rising plateaus of air temperature anomalies at all three stations and two distinct rising plateaus of precipitation anomalies at the YNG and TL stations. Interestingly, the rising plateaus all emerged when the air temperature and precipitation had significantly high WTCs with the streamflow complexity. These results suggest that there is a relationship between climate change and streamflow complexity.

Table 2 provides the multi-year average annual air temperature (MAAT), multi-year average annual precipitation (MAP), average air temperature anomalies (AATA), and average precipitation anomalies (APA) during the two periods with high WTCs. It shows that all the average annual air temperatures at the three stations were relatively low and their anomalies were negative during 1964–1970 and the anomalies of average annual precipitation were also negative. This result suggests that the area experienced a colder and drier process during this period. During 1988–2012, all the average annual air temperatures and the average annual precipitation figures at the three stations were positive and increased from 0.86 to 1.15 °C and 12.2–61.04 mm, respectively. These results suggest that the climate began to be warmer and wetter during 1988–2012.

5. Discussion

The streamflow complexity of the UHR watershed was measured using PE based on 55 years of data on an annual scale. Although many studies have focused on the influence of climate change on streamflow or water availability (Barnett et al., 2005; Naz et al., 2018), few have looked into the impact of climate change on the streamflow complexity. However, the relationship between precipitation and streamflow complexity has been discussed more (Chou, 2014; Huang et al., 2011) though only a limited number have investigated how air temperature change impacts streamflow complexity in inland alpine glacier regions. The results in this paper show that air temperatures also have a critical influence on stream complexity in a glacial alpine watershed.

First, the streamflow complexity was shown to have changed in 1972, which is highly likely to be due to climate change. The changes in streamflow complexity were distinct and, generally, detected in rivers affected by dam constructions (Stosic et al., 2016) and reservoir operations (Zhang et al., 2019a). As there were no large-scale dam constructions in the UHR watershed during the research period or other disturbances of the land use/land cover, this change was likely due to climate change in the region. Several studies have reported variations in the streamflow caused by climate change in the UHR since the 1980s

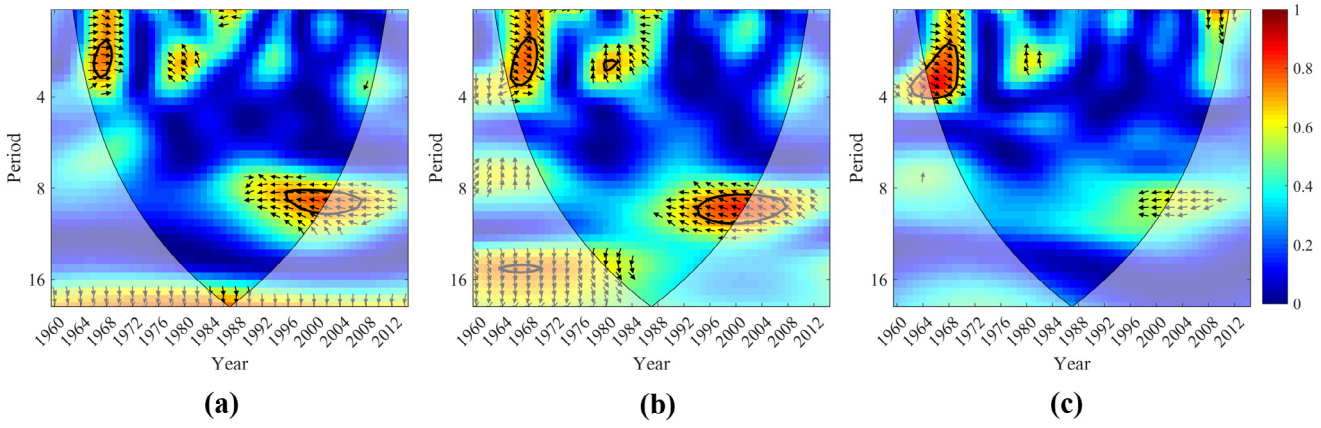

Fig. 4. WTC between the streamflow's complexity and air temperature at QL (a), YNG (b), and TL (c) stations in the UHR watershed.

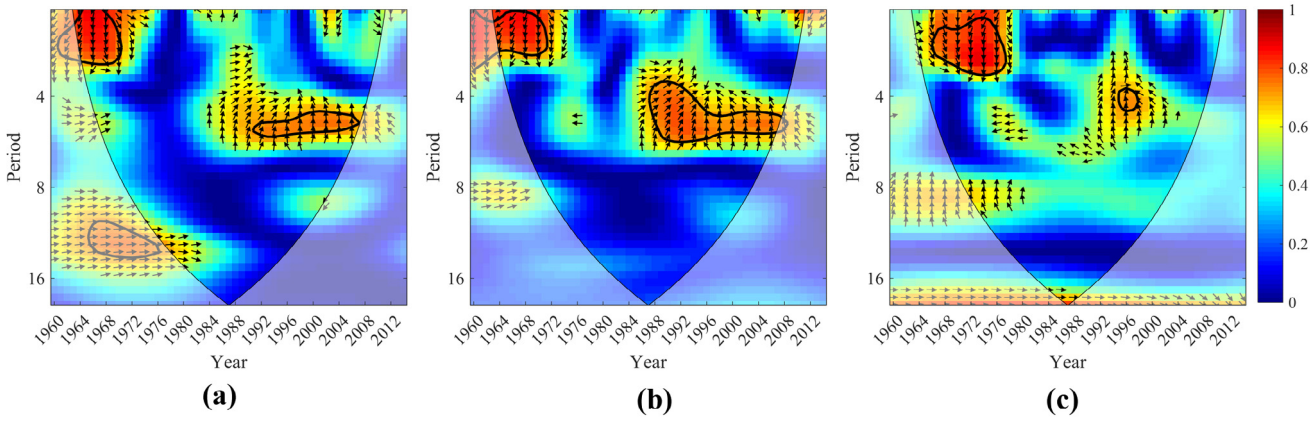

Fig. 5. WTC between the streamflow complexity and the precipitation at QL (a), YNG (b), and TL (c) stations in the UHR watershed.

(Cai et al., 2014; Gao et al., 2018; Luo et al., 2016). Our results also show that after 1972, and especially after 1988, the air temperature and precipitation had long-term significant covariance with the stream complexity. Meanwhile, the air temperature showed an upward trend at the watershed, and precipitation increased (Fig. 6). Therefore, climate change not only altered the volume of streamflow but also played a critical role in changing the streamflow complexity. This find means that the temporal distribution of streamflow also can be altered by climate change. Hence, it is critical for water management agencies of the arid and semi-arid areas, which are very sensitive to the temporal distribution of water resources, to pay attention to the distribution changes of daily streamflow to improve better water resource regulation.

Second, air temperature impacted the streamflow complexity to a weaker degree but across longer timescales than precipitation. The periods of higher air temperature and precipitation began to increase

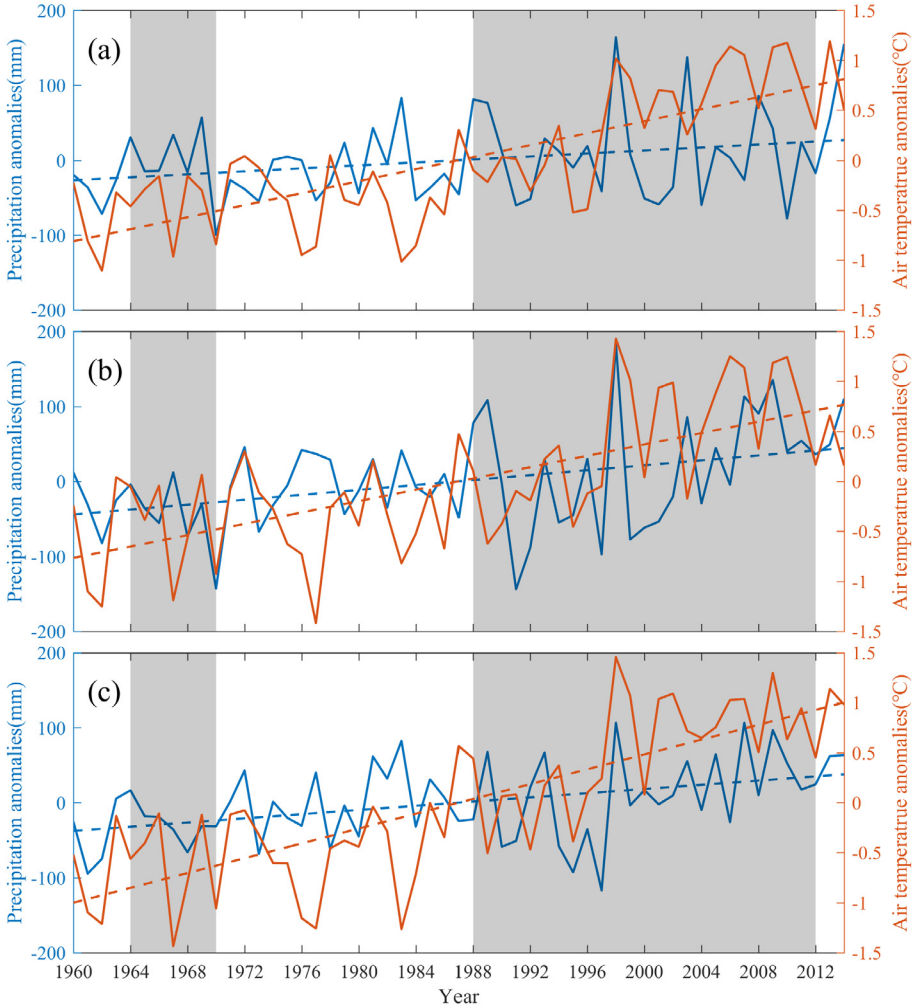

Fig. 6. Interannual variation of the air temperature anomalies (orange) and the precipitation anomalies (blue) of stations QL (a), YNG (c), and TL (c); Dashed lines indicate the linear trends.

Table 2
The characteristics of air temperature and precipitation during 1964–1970 and 1988–2012.

Station	1964–1970				1988–2012			
	MAAT (°C)	AATA (°C)	MAP (mm)	APA (mm)	MAAT (°C)	AATA (°C)	MAP (mm)	APA (mm)
QL	0.73	−0.45	405.67	−3.4	1.60	0.41	417.87	8.79
YNG	−3.27	−0.44	371.70	−47.21	−2.41	0.41	432.74	13.83
TL	−3.12	−0.64	271.33	−26.56	−1.97#	0.51#	307.38	9.50

# indicates no existence of a significant wavelet coherence between air temperature/precipitation and the streamflow complexity.

from around three to four years until they reached record lengths of up to twelve years.

A comparison of the two results of WTCs between air temperature and precipitation on streamflow complexity showed that, although the degree of influence of air temperature significantly increased, it was still relatively weaker than that of precipitation. The complex hydro-meteorological processes may have caused a longer timescale and weaker influence of air temperature in the alpine glacier watershed. Increasing air temperature can affect the streamflow in the UHR in three typical ways: (1) it can accelerate the rate of glacier melting and positively affect the streamflow in glacierized watersheds (Barnett et al., 2005; Bibi et al., 2018); (2) it can lead to permafrost degradation and then affect the streamflow through the increase of base flow (Cuo et al., 2015; Qin et al., 2016); and (3) it can change solid precipitation to liquid precipitation, resulting in a decrease in snowpack and earlier snowmelt (Barnett et al., 2005; Berghuijs et al., 2014; Deng et al., 2017). Since all three are indirect and cover multiple land-surface processes, the impact of air temperature on streamflow complexity is weaker than for precipitation.

Additionally, the clearly weakened WTCs between the air precipitation, the precipitation at the TL station, and the streamflow complexity can be explained from two perspectives. On the one hand, the TL station is located far from the mainstream and tributaries and closer to another sub-watershed, and this could be why the effects of climate variables there decreased after 1988. On the other hand, the extremely low temperatures and low precipitation climate events highly likely caused the significant WTCs between the air temperature, precipitation at the three stations, and the streamflow complexity during 1964–1970. Hence, the significant relationship between the climate variables at the TL station and the complexity of stream is evident for the large-scale extreme climate event.

Notably, the results in this study did not consider all the possible affecting factors for the change of streamflow complexity, such as vegetation variation and land use/land cover change. More influencing factors and their combination with climate change will be discussed in the future. It is important to emphasize that the streamflow complexity showed low WTC with the air temperature, and the precipitation may be caused by the low degree, or slowly developing trend, of climate change from 1972 to 1988.

6. Conclusions

In this study, we applied PE to measure streamflow complexity at the headwaters of the UHR watershed on the northeastern TP. We found that the streamflow complexity in the UHR watershed had significantly increased since 1972 and could be explained by climate change. The increase of streamflow complexity in the headwater area on the TP had not been uncovered in previous studies. Before 1972, periods of low precipitation and very low air temperatures occurred every 3–4 years. However, after 1972, and especially after 1998, greater precipitation and higher air temperatures over longer periods have impacted streamflow complexity. Therefore, climate change has not only altered the streamflow but also increased its complexity. Our results indicate that the dynamic structure and features of streamflow have been transformed by climate change in the UHR watershed and this may well have significance for water resource management agencies and researchers investigating streamflow complexity in other headwater areas across the globe.

CRediT authorship contribution statement

Shi Shen: Conceptualization, Methodology, Software, Data curation, Formal analysis, Writing - original draft, Writing - review & editing. **Changqing Song:** Conceptualization, Investigation, Supervision, Funding acquisition. **Changxiu Cheng:** Conceptualization, Funding acquisition, Writing - review & editing. **Sijing Ye:** Software, Validation.

Declaration of Competing Interest

The authors declare that they have no known competing financial interests or personal relationships that could have appeared to influence the work reported in this paper.

Acknowledgments

We would like to thank the Prof. Zhang Qiang for his constructive suggestions. This work is supported by the National Key Research and Development Plan of China [grant number 2019YFA0606901], the Second Tibetan Plateau Scientific Expedition and Research Program (STEP) [grant number 2019QZKK0608], National Natural Science Foundation of China [grant numbers 41801300, 41901316], the Fundamental Research Funds for the Central Universities [grant number 2019NTST01]. We would also like to thank the Center for Geodata and Analysis, Faculty of Geographical Science, Beijing Normal University (https://gda.bnu.edu.cn/) for their high-performance computing support.

References

Bandt, C., Pompe, B., 2002. Permutation Entropy: A Natural Complexity Measure for Time Series. Phys. Rev. Lett. 88 (17), 174102.
Barnett, T.P., Adam, J.C., Lettenmaier, D.P., 2005. Potential impacts of a warming climate on water availability in snow-dominated regions. Nature 438 (7066), 303–309.
Berghuijs, W.R., Woods, R.A., Hrachowitz, M., 2014. A precipitation shift from snow towards rain leads to a decrease in streamflow. Nat. Clim. Change 4 (7), 583–586.
Bibi, S., et al., 2018. Climatic and associated cryospheric, biospheric, and hydrological changes on the Tibetan Plateau: a review. Int. J. Climatol. 38 (S1), e1–e17.
Brown, L.E., Hannah, D.M., Milner, A.M., 2007. Vulnerability of alpine stream biodiversity to shrinking glaciers and snowpacks. Glob. Change Biol. 13 (5), 958–966.
Büntgen, U., Esper, J., Frank, D.C., Nicolussi, K., Schmidhalter, M., 2005. A 1052-year tree-ring proxy for Alpine summer temperatures. Clim. Dyn. 25 (2), 141–153.
Cai, Y., Huang, W., Teng, F., Gu, S., 2014. Effects of Changing Climate on Glacier Shrinkage and River Flow in the Upper Heihe River Basin, China. J. Coast. Res., 68(sp1): 121-128, 8.
Castillo, A., Castelli, F., Entekhabi, D., 2015. An entropy-based measure of hydrologic complexity and its applications. Water Resour. Res. 51 (7), 5145–5160.
Cazelles, B., et al., 2008. Wavelet analysis of ecological time series. Oecologia 156 (2), 287–304.
Chen, D., et al., 2015. Assessment of past, present and future environmental changes on the Tibetan Plateau (in Chinese). Chin. Sci. Bull. 60 (32), 3025–3035.
Chou, C.-M., 2012. Applying Multiscale Entropy to the Complexity Analysis of Rainfall-Runoff Relationships. Entropy 14 (5), 945–957.
Chou, C.-M., 2014. Complexity analysis of rainfall and runoff time series based on sample entropy in different temporal scales. Stoch. Env. Res. Risk Assess. 28 (6), 1401–1408.

Cuo, L., et al., 2015. Frozen soil degradation and its effects on surface hydrology in the northern Tibetan Plateau. Journal of Geophysical Research: Atmospheres 120 (16), 8276–8298.
Deng, H., Pepin, N.C., Chen, Y., 2017. Changes of snowfall under warming in the Tibetan Plateau. Journal of Geophysical Research: Atmospheres 122 (14), 7323–7341.
Gao, B., et al., 2018. Change in frozen soils and its effect on regional hydrology, upper Heihe basin, northeastern Qinghai-Tibetan Plateau. The Cryosphere 12 (2), 657–673.
Grinsted, A., Moore, J.C., Jevrejeva, S., 2004. Application of the cross wavelet transform and wavelet coherence to geophysical time series. Nonlinear. Processes Geophys. 11 (5/6), 561–566.
Hamed, K.H., Ramachandra Rao, A., 1998. A modified Mann-Kendall trend test for autocorrelated data. J. Hydrol. 204 (1), 182–196.
Hou, Y., Liu, F., Gao, J., Cheng, C., Song, C., 2017. Characterizing Complexity Changes in Chinese Stock Markets by Permutation Entropy. Entropy 19 (10), 514.
Huang, F., et al., 2017. Investigation into Multi-Temporal Scale Complexity of Streamflows and Water Levels in the Poyang Lake Basin. China. Entropy 19 (2), 67.
Huang, F., Xia, Z., Zhang, N., Zhang, Y., Li, J., 2011. Flow-Complexity Analysis of the Upper Reaches of the Yangtze River, China. J. Hydrol. Eng. 16 (11), 914–919.
Huss, M., Hock, R., 2018. Global-scale hydrological response to future glacier mass loss. Nat. Clim. Change 8 (2), 135–140.
Immerzeel, W.W., van Beek, L.P.H., Bierkens, M.F.P., 2010. Climate Change Will Affect the Asian Water Towers. Science 328 (5984), 1382–1385.
Jones, P.D., New, M., Parker, D.E., Martin, S., Rigor, I.G., 1999. Surface air temperature and its changes over the past 150 years. Rev. Geophys. 37 (2), 173–199.
Jovanovic, T., García, S., Gall, H., Mejía, A., 2017. Complexity as a streamflow metric of hydrologic alteration. Stoch. Env. Res. Risk Assess. 31 (8), 2107–2119.
Kendall, M.G., 1975. Rank correlation methods. Charles Griffin, London, England.
Krasovskaia, I., 1995. Quantification of the stability of river flow regimes. Hydrol. Sci. J. 40 (5), 587–598.
Kuang, X., Jiao, J.J., 2016. Review on climate change on the Tibetan Plateau during the last half century. J. Geophys. Res.: Atmosph. 121 (8), 3979–4007.
Liu, J., Zhang, Q., Feng, S., Gu, X., Singh, V.P., Sun, P., 2019. Global Attribution of Runoff Variance Across Multiple Timescales. J. Geophys. Res. Atmosph. 124.
Liu, J., Zhang, Q., Singh, V.P., Shi, P., 2017. Contribution of multiple climatic variables and human activities to streamflow changes across China. J. Hydrol. 545, 145–162.
Liu, J., Zhang, Q., Song, C., Zhang, Y., Sun, P., Gu, X., 2018. 2018, Hydrological effects of climate variability and vegetation dynamics on annual fluvial water balance in global large river basins. Hydrol. Earth Syst. Sci. 22 (7), 4047–4060.
Li, Z., Zhang, Y.K., 2008. Multi-scale entropy analysis of Mississippi River flow. Stoch. Env. Res. Risk Assess. 22 (4), 507–512.
Luo, K., Tao, F., Moiwo, J.P., Xiao, D., 2016. Attribution of hydrological change in Heihe River Basin to climate and land use change in the past three decades. Sci. Rep. 6, 33704.
Luo, M., Pan, C., Zhan, C., 2019. Diagnosis of Change in Structural Characteristics of Streamflow Series Based on Selection of Complexity Measurement Methods: Fenhe River Basin, China. J. Hydrol. Eng. 24 (2), 05018028.
Mann, H.B., 1945. Nonparametric Tests Against Trend. Econometrica 13 (3), 245.
Mihailović, D.T., et al., 2019. Analysis of daily streamflow complexity by Kolmogorov measures and Lyapunov exponent. Physica A: Statist. Mechan. Appl. 525, 290–303.
Mihailović, D.T., Nikolić-Đorić, E., Drešković, N., Mimić, G., 2014. Complexity analysis of the turbulent environmental fluid flow time series. Physica A: Statist. Mechan. Appl. 395, 96–104.
Milly, P.C.D., Dunne, K.A., Vecchia, A.V., 2005. Global pattern of trends in streamflow and water availability in a changing climate. Nature 438, 347.
Naz, B.S., et al., 2018. Effects of climate change on streamflow extremes and implications for reservoir inflow in the United States. J. Hydrol. 556, 359–370.
Oki, T., Kanae, S., 2006. Global Hydrological Cycles and World Water Resources. Science 313, 1068–1072.
Pan, F., Pachepsky, Y.A., Guber, A.K., McPherson, B.J., Hill, R.L., 2012. Scale effects on information theory-based measures applied to streamflow patterns in two rural watersheds. J. Hydrol. 414–415, 99–107.
Pande, S., Moayeri, M., 2018. Hydrological Interpretation of a Statistical Measure of Basin Complexity. Water Resour. Res. 54 (10), 7403–7416.
Parajka, J., et al., 2013. Comparative assessment of predictions in ungauged basins – Part 1: Runoff-hydrograph studies. Hydrol. Earth Syst. Sci. 17 (5), 1783–1795.
Qin, Y., et al., 2016. Long-term change in the depth of seasonally frozen ground and its ecohydrological impacts in the Qilian Mountains, northeastern Tibetan Plateau. J. Hydrol. 542, 204–221.
Ribeiro, H.V., Zunino, L., Mendes, R.S., Lenzi, E.K., 2012. Complexity–entropy causality plane: A useful approach for distinguishing songs. Physica A: Statist. Mechan. Appl. 391 (7), 2421–2428.
Sang, Y.-F., Wang, D., Wu, J.-C., Zhu, Q.-P., Wang, L., 2009. The relation between periods' identification and noises in hydrologic series data. J. Hydrol. 368 (1), 165–177.
Sang, Y.-F., Wang, D., Wu, J.-C., Zhu, Q.-P., Wang, L., 2011. Wavelet-Based Analysis on the Complexity of Hydrologic Series Data under Multi-Temporal Scales. Entropy 13 (1), 195–210.
Sang, Y.-F., Wang, Z., Liu, C., 2014. Comparison of the MK test and EMD method for trend identification in hydrological time series. J. Hydrol. 510, 293–298.
Sen, A.K., 2009. Complexity analysis of riverflow time series. Stoch. Env. Res. Risk Assess. 23 (3), 361–366.
Serinaldi, F., Zunino, L., Rosso, O.A., 2014. Complexity–entropy analysis of daily stream flow time series in the continental United States. Stoch. Env. Res. Risk Assess. 28 (7), 1685–1708.
Sharifi, E., Steinacker, R., Saghafian, B., 2018. Multi time-scale evaluation of high-resolution satellite-based precipitation products over northeast of Austria. Atmos. Res. 206, 46–63.
Singh, P., Bengtsson, L., 2005. Impact of warmer climate on melt and evaporation for the rainfed, snowfed and glacierfed basins in the Himalayan region. J. Hydrol. 300 (1), 140–154.
Singh, V.P., 1997. The use of entropy in hydrology and water resources. Hydrol. Process. 11 (6), 587–626.
Singh, V.P., 2011. Hydrologic Synthesis Using Entropy Theory: Review. J. Hydrol. Eng. 16 (5), 421–433.
Sivakumar, B., 2009. Nonlinear dynamics and chaos in hydrologic systems: latest developments and a look forward. Stoch. Env. Res. Risk Assess. 23 (7), 1027–1036.
Sivakumar, B., Singh, V.P., 2012. Hydrologic system complexity and nonlinear dynamic concepts for a catchment classification framework. Hydrol. Earth Syst. Sci. 16 (11), 4119–4131.
Srivalli, C.N.S., Jothiprakash, V., Sivakumar, B., 2019. Complexity of streamflows in the west-flowing rivers of India. Stoch. Env. Res. Risk Assess. 33 (3), 837–853. https://doi.org/10.1007/s00477-019-01665-3.
Stosic, T., Telesca, L., de Souza Ferreira, D.V., Stosic, B., 2016. Investigating anthropically induced effects in streamflow dynamics by using permutation entropy and statistical complexity analysis: A case study. J. Hydrol. 540, 1136–1145.
Su, L., Miao, C., Borthwick, A.G.L., Duan, Q., 2017. Wavelet-based variability of Yellow River discharge at 500-, 100-, and 50-year timescales. Gondwana Res. 49, 94–105.
Torrence, C., Compo, G.P., 1998. A Practical Guide to Wavelet Analysis. Bull. Am. Meteorol. Soc. 79 (1), 61–78.
Torrence, C., Webster, P.J., 1999. Interdecadal Changes in the ENSO–Monsoon System. J. Clim. 12 (8), 2679–2690.
Wang, J., Li, H., Hao, X., 2010. Responses of snowmelt runoff to climatic change in an inland river basin, Northwestern China, over the past 50 years. Hydrol. Earth Syst. Sci. 14 (10), 1979–1987.
Wang, Q., et al., 2017. Hydro-thermal processes and thermal offsets of peat soils in the active layer in an alpine permafrost region, NE Qinghai-Tibet plateau. Global Planet. Change 156, 1–12.
Wang, Q., Zhang, T., Peng, X., Cao, B., Wu, Q., 2015. Changes of Soil Thermal Regimes in the Heihe River Basin Over Western China. Arct. Antarct. Alp. Res. 47 (2), 231–241.
Wang, X., Yang, T., Xu, C.-Y., Yong, B., Shi, P., 2019. Understanding the discharge regime of a glacierized alpine catchment in the Tianshan Mountains using an improved HBV-D hydrological model. Global Planet. Change 172, 211–222.
Wang, Y., Feng, Q., Kang, X., 2016. Tree-ring-based reconstruction of temperature variability (1445–2011) for the upper reaches of the Heihe River Basin, Northwest China. J. Arid Land 8 (1), 60–76.
Wang, Y., et al., 2020. Quantifying the change in streamflow complexity in the Yangtze River. Environ. Res. 180, 108833.
Wulf, H., Bookhagen, B., Scherler, D., 2016. Differentiating between rain, snow, and glacier contributions to river discharge in the western Himalaya using remote-sensing data and distributed hydrological modeling. Adv. Water Resour. 88, 152–169.
Xu, X., Lu, C., Shi, X., Gao, S., 2008. World water tower: An atmospheric perspective. Geophys. Res. Lett. 35 (20).
You, Q., Min, J., Kang, S., 2016. Rapid warming in the Tibetan Plateau from observations and CMIP5 models in recent decades. Int. J. Climatol. 36 (6), 2660–2670.
Zanin, M., Zunino, L., Rosso, O.A., Papo, D., 2012. Permutation Entropy and Its Main Biomedical and Econophysics Applications: A Review. Entropy 14 (8), 1553–1577.
Zhang, J., Xiao, H., Zhang, X., Li, F., 2019a. Impact of reservoir operation on runoff and sediment load at multi-time scales based on entropy theory. J. Hydrol. 569, 809–815.
Zhang, D., Liu, X., Zhang, Q., Liang, K., Liu, C., 2016. Investigation of factors affecting intra-annual variability of evapotranspiration and streamflow under different climate conditions. J. Hydrol. 543, 759–769.
Zhang, Q., Liu, J., Singh, V.P., Shi, P., Sun, P., 2017. Hydrological responses to climatic changes in the Yellow River basin, China: climatic elasticity and streamflow prediction. J. Hydrol. 554, 635–645.
Zhang, Q., Zhou, Y., Singh, V.P., Chen, X., 2012. The influence of dam and lakes on the Yangtze River streamflow: long-range correlation and complexity analyses. Hydrol. Process. 26 (3), 436–444.
Zhang, T., Cheng, C., Gao, P., 2019b. Permutation Entropy-Based Analysis of Temperature Complexity Spatial-Temporal Variation and Its Driving Factors in China. 21(10): 1001.
Zhong, F., Cheng, Q., Ge, Y., 2019. Relationships between Spatial and Temporal Variations in Precipitation, Climatic Indices, and the Normalized Differential Vegetation Index in the Upper and Middle Reaches of the Heihe River Basin, Northwest China. Water 11 (7), 1394.
Zhong, L., Su, Z., Ma, Y., Salama, M.S., Sobrino, J.A., 2011. Accelerated Changes of Environmental Conditions on the Tibetan Plateau Caused by Climate Change. J. Clim. 24 (24), 6540–6550.
Zhou, Y., Zhang, Q., Li, K., Chen, X., 2012. Hydrological effects of water reservoirs on hydrological processes in the East River (China) basin: complexity evaluations based on the multi-scale entropy analysis. Hydrol. Process. 26 (21), 3253–3262.
Zunino, L., Zanin, M., Tabak, B.M., Pérez, D.G., Rosso, O.A., 2009. Forbidden patterns, permutation entropy and stock market inefficiency. Phys.A: Statist. Mechan. Appl. 388 (14), 2854–2864.